Electronic Supplementary Material (ESI) for Chemical Communications

Supporting information

Utilizing the Tb^{3+} as energy transfer bridge to connect the Eu^{2+}-Sm^{3+} luminescent centers: Realization the Efficient Sm^{3+} Ion Red Emission under near-UV Excited

Yongchao Jia,[a,b] Wei Lü,[a] Ning Guo,[a,b] Wenzhen Lü,[a,b] Qi Zhao,[a,b] Hongpeng You [a,*]

[a]*State key Laboratory of Rare Earth Resource Utilization, Changchun Institute of Applied Chemistry, Chinese Academy of Sciences, Changchun 130022, P. R. China.*

[b]*Graduate University of the Chinese Academy of Sciences, Beijing 100049, P. R. China.*

Experimental Section

$SrCO_3$ (Analytical Reagent, A. R.), Y_2O_3 (99.99%), Eu_2O_3 (99.99%), Tb_4O_7 (99.99%), Sm_2O_3 (99.99%), $NH_4H_2PO_4$ (Analytical Reagent, A. R.), were used as the raw materials.

The phosphors with the compositions:

$Sr_{2.98}Y(PO_4)_3$:$0.02Eu^{2+}$ (SYPO:Eu^{2+});

$Sr_3Y_{2.99}(PO_4)_3$:$0.01Sm^{3+}$ (SYPO:Sm^{3+});

$Sr_3Y_{2.99}(PO_4)_3$:$0.01Tb^{3+}$ (SYPO:Tb^{3+});

$Sr_{2.98}Y_{1-x}(PO_4)_3$:$0.02Eu^{2+}$,xSm^{3+} (SYPO:$0.02Eu^{2+}$,xSm^{3+});

$Sr_{2.98}Y_{1-x}(PO_4)_3$:$0.02Eu^{2+}$,xTb^{3+} (SYPO:$0.02Eu^{2+}$,xTb^{3+});

$Sr_3Y_{0.1-x}(PO_4)_3$:$0.9Tb^{3+}$,xSm^{3+} (SYPO:$0.9Tb^{3+}$,xSm^{3+});

$Sr_{2.98}Y_{1-x}(PO_4)_3$:$0.02Eu^{2+}$,$0.9Tb^{3+}$,xSm^{3+} (SYPO:$0.02Eu^{2+}$,$0.9Tb^{3+}$,xSm^{3+}); were prepared using high temperature solid-state reaction method. The stoichiometric amount of raw materials was thoroughly mixed by grinding in an agate mortar. The power mixtures were then transferred into crucibles and heated at 1300°C for 4 h in crucibles alone with the air. After that, the sample was reground in a mortar followed by sintering under a reductive atmosphere at 1200°C for 2 h in a 10% H_2-90%N_2 gas mixture. Finally, the obtained samples were cooled to room temperature and ground again in an agate mortar.

Characterization

Powder XRD data were obtained using Cu-K radiation (Bruker D8) over the angular range 10°≤2θ≤80° with a step size 0.02°. Room temperature photoluminescence (PL) spectra

were measured on Hitachi F-4500 luminescence spectrophotometer scanning the wavelength range of 300-700nm. The diffuse-reflectance spectra were obtained by a SHIMADZU UV-3600 UV-vis-NiR spectrophotometer with the reflection of black felt (reflection 3%) and white $BaSO_4$ (reflection100%) in the wavelength region of 200–600 nm. The luminescence decay curve was obtained from a Lecroy Wave Runner 6100 Digital Oscilloscope (1GHz) using a tunable laser (puls width = 4ns, gate = 50ns) as the excitation source (Continum Sunlite OPO). All the measurements mentioned above were performed at room temperature.

Results and Discussion

1. Analysis of the sensitization effect of the Eu^{2+}-Tb^{3+}, Tb^{3+}-Sm^{3+} luminescent centers

Figure S5 shows the emission spectra of SrYPO:0.02Eu^{2+},xTb^{3+} under 365 nm excitation. With increasing Tb^{3+} content, the intensity of green emission lines increase systematically. Meanwhile, a remarkable drop of Eu^{2+} emission band is seen from x = 0.1 to 0.9. Figure S6 depicted the PL decay curves of Eu^{2+} ions in SrYPO:0.02Eu^{2+},xTb^{3+}, which were measured with an excitation at 355 nm and monitored at 520 nm. The decay curve for singly Eu^{2+}-doped SrYPO host can be fitted into a second-exponential function. The incorporation of Tb^{3+} ions can significantly modifies the fluorescent dynamics of the Eu^{2+} ions. When Tb^{3+} ions were introduced, the fluorescence decays of Eu^{2+} ions deviate slightly from a second-exponential rule. This deviation is more evident with the increase in the content of Tb^{3+} ions. Above facts provide the solid evidence for sensitization effect between the Eu^{2+}-Tb^{3+} luminescent centers.

Figure S7 shows the emission spectra of SrYPO:0.9Tb^{3+},xSm^{3+} under 381 nm excitation. With increasing Sm^{3+} content, the intensity of red emission lines reaches a maximum as x equals about 0.02 and then begins to decrease due to concentration quenching. Meanwhile, a remarkable drop of Tb^{3+} emission lines is seen from x = 0.01 to 0.07. Figure S8 depicted the PL decay curves of Tb^{3+} ions in SrYPO:0.9Tb^{3+},xSm^{3+}, which were measured with an excitation at 355 nm and monitored at 542 nm. The decay curve for singly Tb^{3+}-doped SrYPO host can be fitted into a single-exponential function. The incorporation of Sm^{3+} ions can significantly modifies the fluorescent dynamics of the Tb^{3+} ions. When Sm^{3+} ions were introduced, the fluorescence decays of Tb^{3+} ions deviate slightly from a single-exponential rule. This deviation is more evident with the increase in the content of Sm^{3+} ions. Above facts provide the solid

evidence for sensitization effect between the Tb^{3+}-Sm^{3+} luminescent centers.

2. Phase formation

Figure S10 shows the XRD patterns of the typical obtained powders, together with the standard data for SLnPO (Ln = Y, Tb). All the diffraction peaks of obtained samples can be indexed to the corresponding standard data, indicating that obtained samples are single phase and doped Eu^{2+}/Sm^{3+} ions have been incorporated in the host lattice by replace Sr^{2+}/Ln^{3+} crystallographic sites.

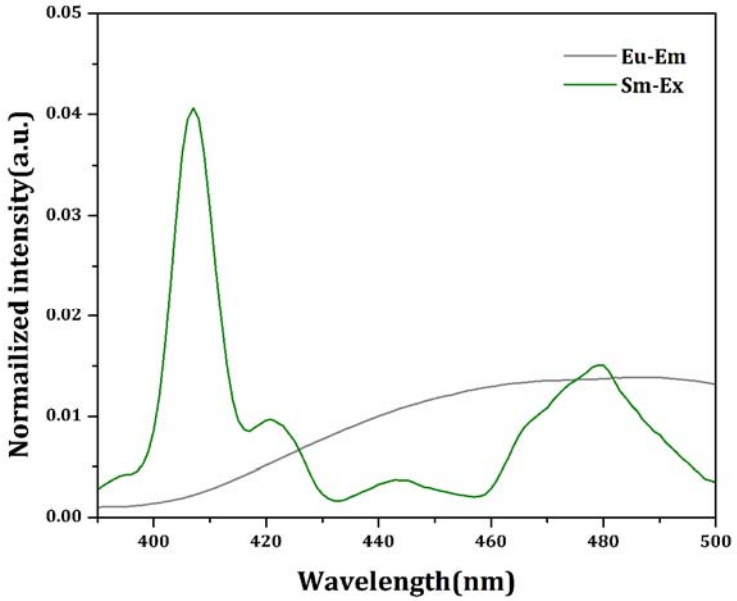

Figure S1. The overlap spectra between the PLE-SYPO:0.02Sm^{3+} and PL-SYPO:0.02Eu^{2+} samples.

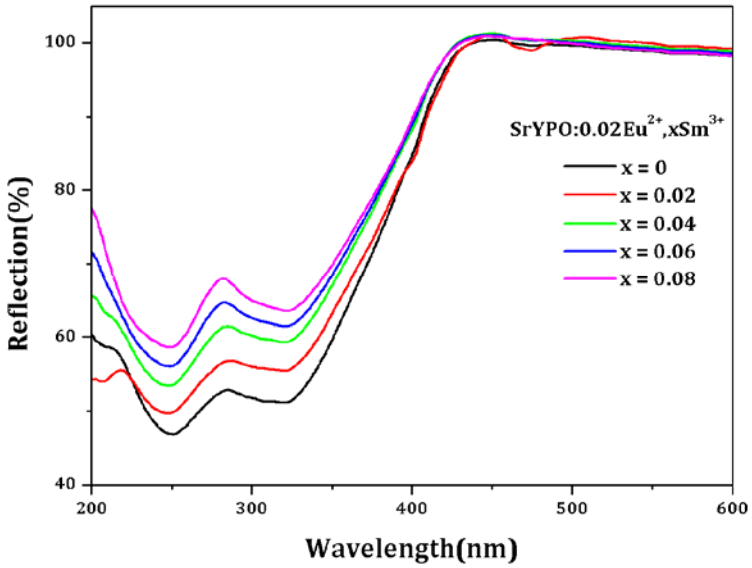

Figure S2. Diffuse reflection spectra of SrYPO:0.02Eu^{2+},xSm^{3+} samples (x = 0, 0.02, 0.04, 0.06, 0.08).

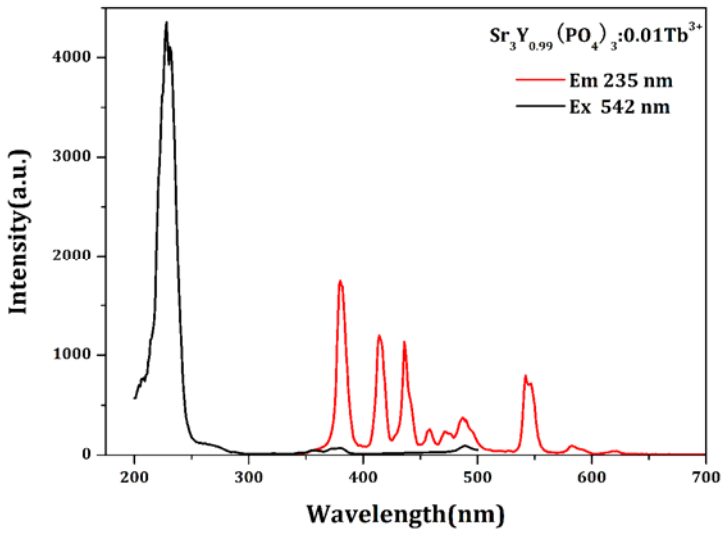

Figure S3. The PL and PLE of the SYPO:0.01Tb^{3+} sample.

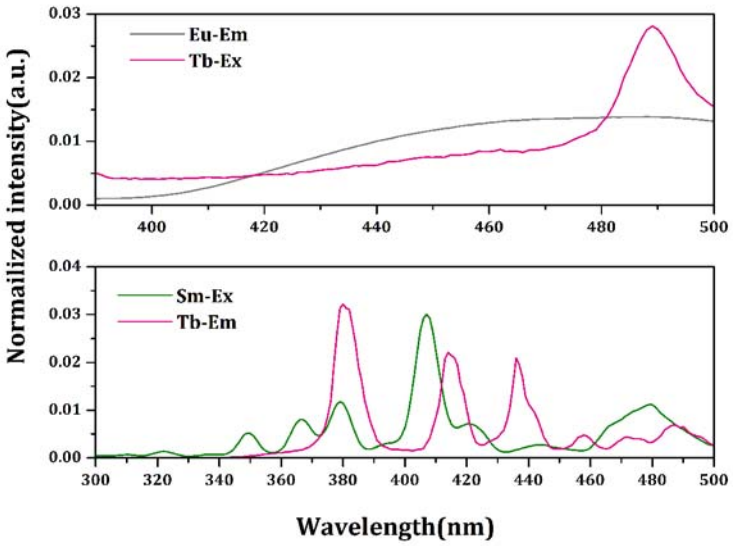

Figure S4. The overlap spectra between the PLE-SYPO:0.01Tb^{3+} and PL-SYPO:0.02Eu^{2+} samples; the PLE-SYPO:0.02Sm^{3+} and PL-SYPO:0.01Tb^{3+} samples.

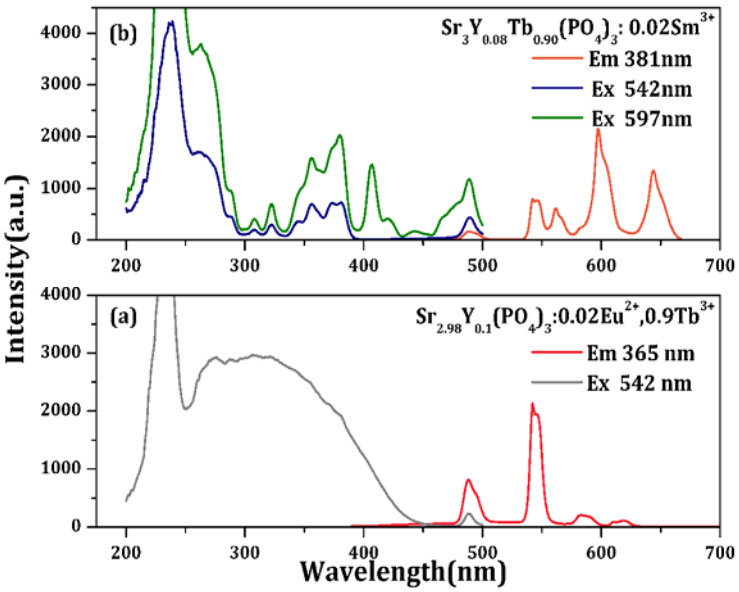

Figure S5. The PL and PLE of the Eu^{2+}/Tb^{3+} codoped SYPO sample (a); the Tb^{3+}/Sm^{3+} codoped SYPO sample (b).

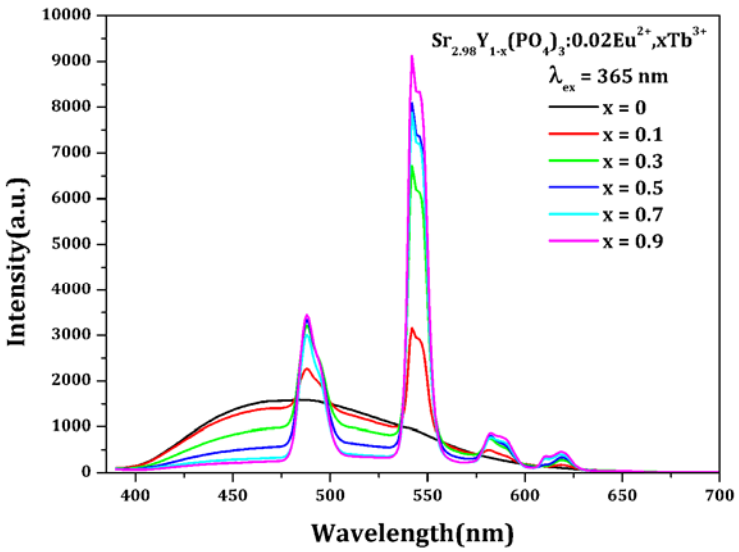

Figure S6. The PL spectra of SYPO:0.02Eu^{2+},xTb^{3+} (x = 0, 0.1, 0.3, 0.5, 0.7, 0.9) samples under the 365 nm excitation.

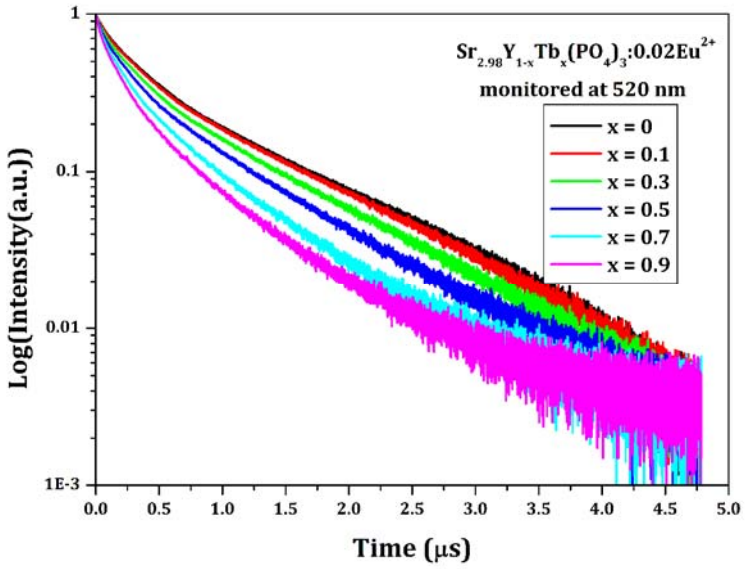

Figure S7. Decay curves of Eu^{2+} ions in SYPO:0.02Eu^{2+},xTb^{3+} (x = 0, 0.1, 0.3, 0.5, 0.7, 0.9) samples (excited at 355 nm, monitored at 520 nm).

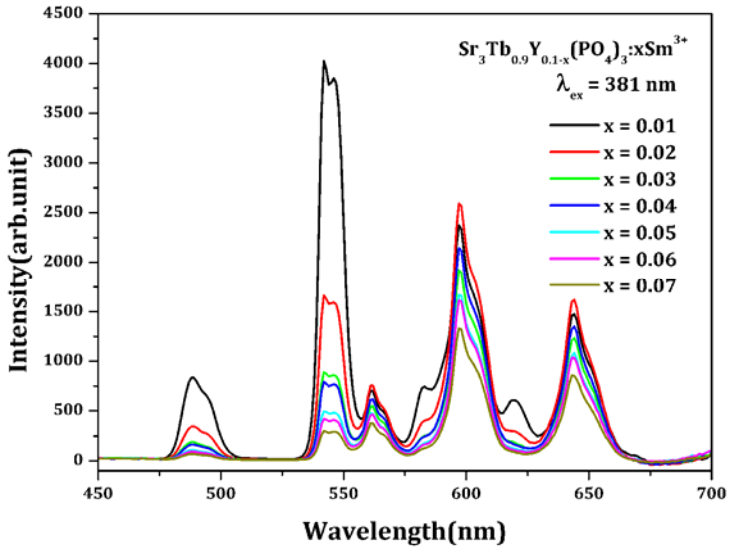

Figure S8. The PL spectra of SYPO:0.9Tb^{3+},xSm^{3+} (x = 0, 0.01, 0.02, 0.03, 0.04, 0.05, 0.06, 0.07,) samples under the 381 nm excitation.

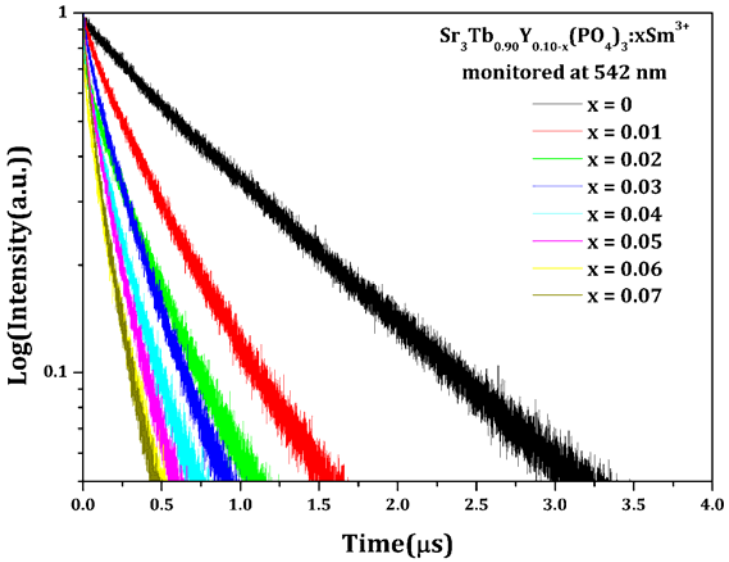

Figure S9. Decay curves of Tb^{3+} ions in SYPO:0.9Tb^{3+},xSm^{3+} (x = 0, 0.01, 0.02, 0.03, 0.04, 0.05, 0.06, 0.07,) samples (excited at 355 nm, monitored at 542 nm).

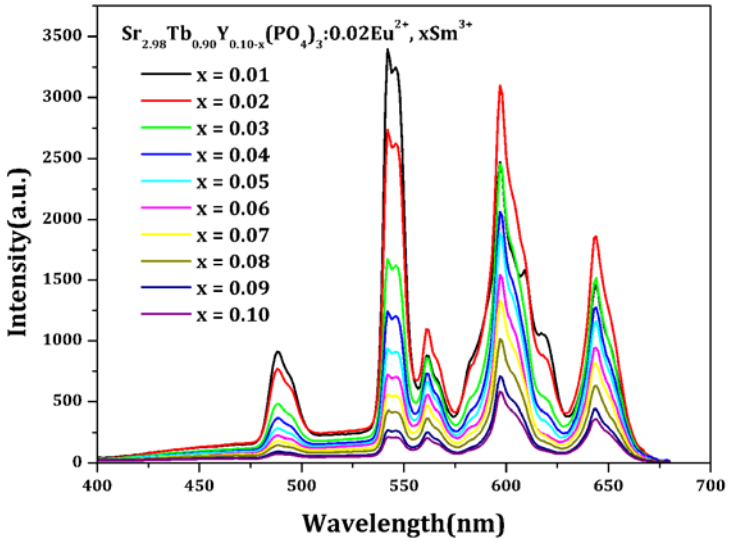

Figure S10. The PL spectra of SYPO:0.02Eu^{2+},0.9Tb^{3+},xSm^{3+} (x = 0, 0.01, 0.02, 0.03, 0.04, 0.05, 0.06, 0.07,) samples under the 390 nm excitation.

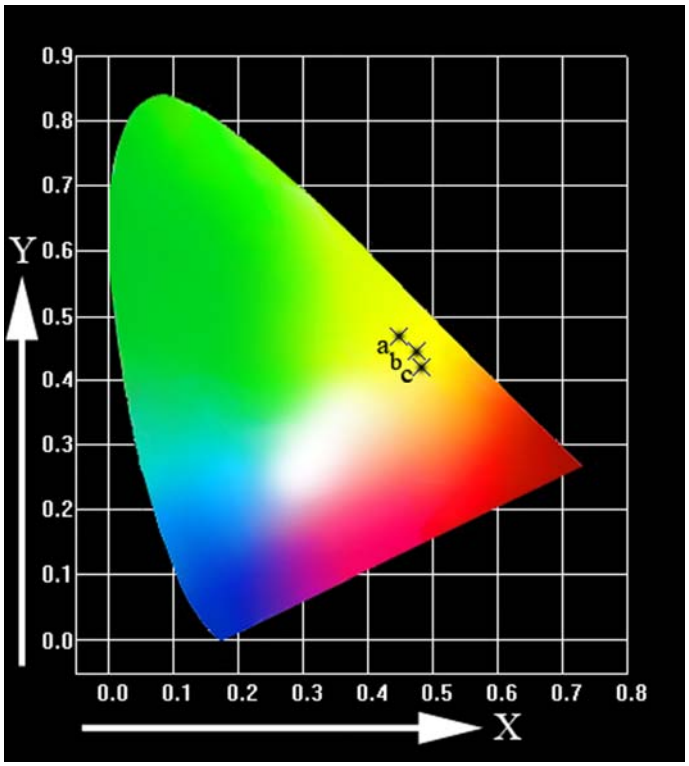

Figure S11. CIE chromaticity diagram for SYPO:0.02Eu^{2+},0.9Tb^{3+},xSm^{3+} excited at 390 nm: (a) x = 0.01; (b) x = 0.05; (c) x = 0.10.

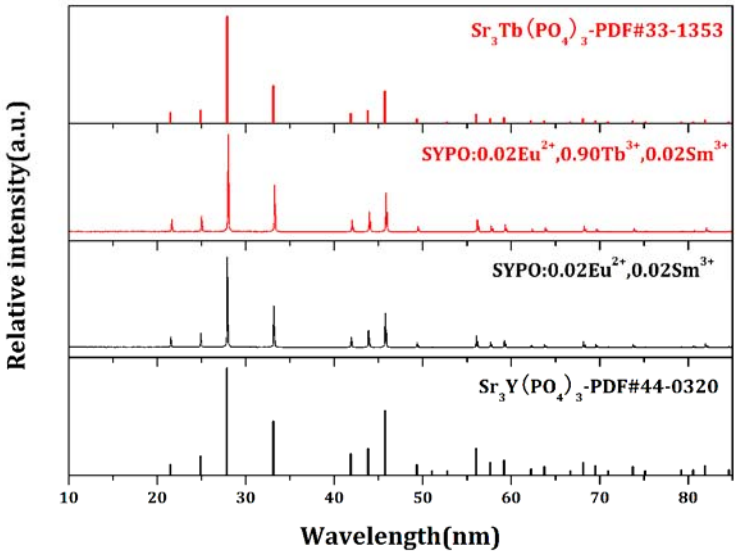

Figure S12. XRD profiles for the typical powders SYPO:0.02Eu^{2+},0.02Sm^{3+} and SrYPO:0.02Eu^{2+},0.90Tb^{3+},0.02Sm^{3+}. The standard data for $Sr_3Y(PO_4)_3$ (JCPDS card No. 44-0320) and $Sr_3Tb(PO_4)_3$ (JCPDS card No. 33-1535) is shown as reference.